# Experimental study of nucleate pool boiling heat transfer to ammonia–water–lithium bromide solution

A. Sathyabhama [a,*], T.P. Ashok Babu [b,1]

[a] Dept. of Mech. Engg. NITK, Surathkal/Faculty, MSRIT, Vidya Soudha, MSR Nagar, MSRIT Post, Bangalore 560 054, Karnataka, India
[b] Dept. of Mech. Engg. NITK, Surathkal Post Srinivasnagar, Mangalore 575 025, Karnataka, India

ABSTRACT

Visualization of bubble nucleation during nucleate pool boiling outside a vertical cylindrical heated surface was done for ammonia–water binary and ammonia–water–lithium bromide ternary mixture in order to obtain a descriptive behavior of the boiling which was directly compared with the measured heat transfer coefficient at low pressure of 4–8 bar and at low ammonia mass fraction of $0 < x_{NH_3} < 0.3$ and at different heat flux. The lithium bromide concentration of the solution was chosen in the range of 10–50% of mass ratio of lithium bromide in pure water. The effect of concentrations, heat flux and pressure on boiling heat transfer coefficient was studied. Still images taken with high speed camera are used to demonstrate the increase in boiling heat transfer coefficient with the addition of lithium bromide salt to ammonia–water mixture. Further work is required to obtain quantitative information about bubble nucleation parameters.

© 2011 Elsevier Inc. All rights reserved.

## 1. Introduction

Absorption refrigeration systems have attracted increasing research interests in recent years. Unlike mechanical vapor compression refrigerators, these systems cause no ozone depletion and reduce demand on electricity supply. Besides, heat powered systems could be superior to electricity powered systems in that they harness inexpensive waste heat, solar, biomass or geothermal energy sources for which the cost of supply is negligible in many cases. This makes heat powered refrigeration a viable and economic option. The most common absorption systems are $H_2O$–LiBr and $NH_3$–$H_2O$ cycles.

The $NH_3$–$H_2O$ pair possesses very good heat and mass transfer characteristics but requires rectification to remove water vapor from the ammonia rich refrigerant vapor. Lithium bromide, on the other hand, is a non-volatile salt that can act as an absorber for both ammonia as well as water due to ion formation and complexing. Therefore, ternary $NH_3$–$H_2O$–LiBr mixtures with high salt concentrations could offer better performance by absorbing ammonia and water thus reducing rectification losses, especially at higher operating temperatures.

The thermodynamic properties of the $NH_3$–$H_2O$–LiBr system (principally for a LiBr/$H_2O$ ratio of 60/40 weight percent) have been investigated by Radermacher [1]. McLinden and Radermacher [2] compared the performance of an absorption heat pump operating with $NH_3$–$H_2O$ and $NH_3$–$H_2O$–LiBr mixtures. Although the COP of the heat pump operating with ternary mixture was lower than with the binary system, there were indications of lower water content in the refrigerant vapor entering the rectifier with the ternary mixture.

Peters et al. [3,4] investigated the effects of lithium bromide on the $NH_3$–$H_2O$ system using a static method to measure vapor–liquid equilibrium data of $NH_3$–$H_2O$–LiBr mixtures over temperatures between 303.15 and 423.15 K, and pressures up to 1.5 MPa. They reported reduction in partial pressure of both ammonia and water in the vapor phase compared to respective pressures in binary $NH_3$–$H_2O$ system. They developed a quasi-chemical reaction model to correlate experimental data. The correlation was in good agreement with the experimental data.

Yuyuan et al. [5] measured vapor–liquid equilibrium (VLE) data for $NH_3$–$H_2O$–LiBr system at 10 temperature points between 15 and 85 °C, and pressures up to 2 MPa. The LiBr concentration of the solution was chosen in the range of 5–60% of mass ratio of LiBr in pure water. The VLE for the $NH_3$–$H_2O$–LiBr ternary solution was measured statically. It was seen that at the same temperature and ammonia concentration, vapor pressure of ternary $NH_3$–$H_2O$–LiBr mixture solution was lower than that of the binary $NH_3$–$H_2O$ solution. The ammonia content in the vapor phase of ternary $NH_3$–$H_2O$–LiBr mixture solution was higher than that in the binary $NH_3$–$H_2O$ solution without lithium bromide.

* Corresponding author. Fax: +91 080 23603124.
E-mail address: sathyabhamaa@hotmail.com (A. Sathyabhama).
[1] Fax: +91 0824 2474033.

vapor liquid equilibria of the $NH_3$–$H_2O$–LiBr system have been established, no information however, is available on the effect of dissolved salt on the boiling heat transfer which is indispensable in the design of these systems. The aim of the present paper is to obtain the nucleate pool boiling heat transfer coefficient of $NH_3$–$H_2O$–LiBr ternary system at different mass fraction of ammonia and lithium bromide, at different pressure and at different heat flux. The present investigation also aims at obtaining a visual record of nucleation to study the effect of lithium bromide on bubble parameters.

Boiling heat transfer has been intensively investigated, but it is not yet possible to predict heat transfer coefficients with the accuracy necessary for reliable design of generators/evaporators, particularly, for the boiling of mixtures. Most boiling research has been limited to the behavior of pure components or binary mixtures. Empirical or semi-empirical correlations have been proposed to correlate the heat transfer coefficients. Most correlations represent quite well the experimental data they were developed from, but large discrepancy occurs when they are applied to other data.

There have been relatively few studies on the boiling heat transfer of ammonia/water mixture. Inoue et al. [6], measured the pool boiling heat transfer coefficients of ammonia/water mixture and its pure components on a horizontal platinum wire (diameter of 0.3 mm, 37 mm length) at the pressure of 0.4–0.7 MPa with heat flux varying from 0.4 to 1.5 MW/m$^2$ and the mass fraction from 0 to 1. Arima et al. [7], obtained data on a horizontal flat circular surface of silver with a diameter of 10 mm for ammonia/water mixture and its pure components at a pressure level from 1 to 15 bar with heat flux varying from 0.1 to 2.0 MW/m$^2$. It was found by both the authors that the mixture in the range of the mass fraction, 0.2–0.9 gives smaller heat transfer coefficients than its individual components.

Many other previous experimental investigations have also revealed a reduction of heat transfer coefficients in nucleate boiling of mixtures, compared with those for a single component substance of the same physical properties as the mixture, or compared with the linearly interpolated values between the two pure components comprising the mixture. Some physical explanations for the reduction were suggested and reviewed (Fujita and Tsutsui [8]). Deterioration in the heat transfer of mixtures has been recently clarified, but there are few reports on the heat transfer enhancement of binary mixtures. Inoue et al. [9] studied the effect of cationic surfactant on boiling heat transfer enhancement of ethanol/water mixture. They reported increase in boiling heat transfer coefficient in low heat flux range in low ethanol fraction range by the surfactant. They attributed this increase to the decrease in surface tension of the mixture by the addition of surfactant.

The information available on the boiling of inorganic salt solution is very less compared to that available on organic liquid mixtures. Boiling characteristics of aqueous electrolyte solutions are likely to be different from those of organic mixtures because of the differences in surface tension, wetting characteristics and bubble coalescence and breakup behavior (Jamialahmadi et al. [10]). Considerable decrease in heat transfer coefficient at low heat fluxes were observed by Jamialahmadi et al. for aqueous salt solutions. At high heat fluxes the negative effect of the dissolved electrolyte gradually decreased and finally some improvement in heat transfer coefficient was observed.

## 2. Experimental setup

The schematic diagram of experimental setup is shown in Fig. 1. The unit consists of boiling vessel, water pump, vacuum pump, condenser coil and test section. Boiling vessel 80 mm diameter and 200 mm long made up of SS 316 is fitted with SS 316 flanges at the top and at the bottom as shown in Fig. 1. The vessel is fitted with two sight glasses to observe and record the boiling phenomena. The top flange has provisions for liquid charging, condenser cooling water inlet and outlet, vacuum pump, pressure transducer and thermocouples to measure liquid and vapor temperatures. Bottom flange has provisions for heater rod and drain. The cylindrical stainless steel heater rod of 6 mm diameter and a heating length of 20 mm is mounted vertically within the boiling vessel and is completely immersed in the liquid pool. Boiling takes place
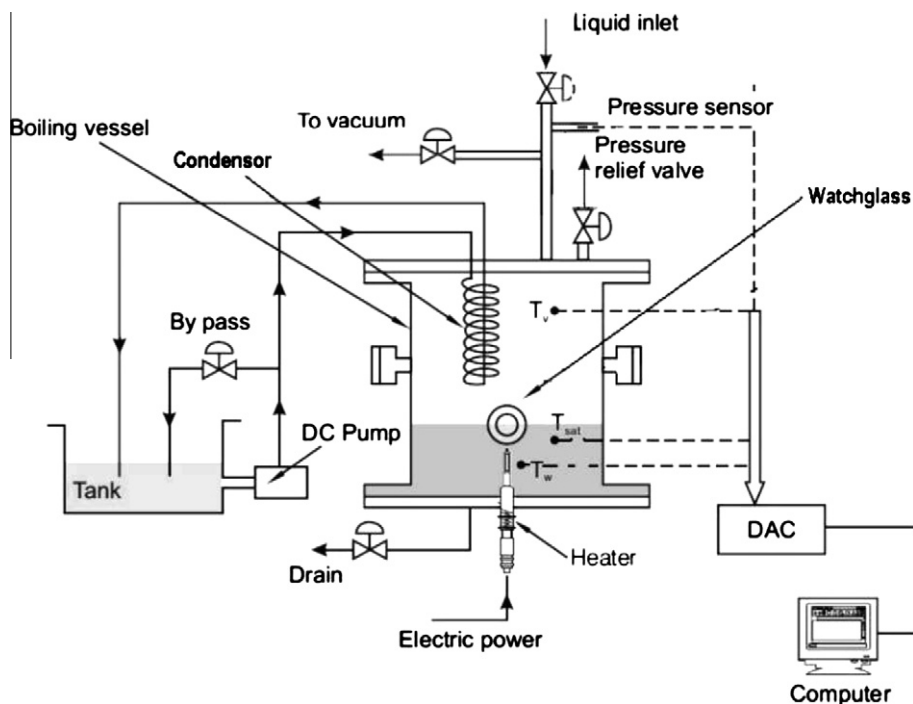


**Fig. 1.** Schematic diagram of experimental setup.

on the outer surface of this heater rod. The test surface is heated by an electrical heating element of 1 kW capacity. The heating element is connected to a wattmeter through a dimmerstat to read the power supplied to it. The details of the test heater are given in Fig. 2.

All temperatures of the system are measured using chrome alumel K type thermocouples. Two thermocouples are set in the liquid pool and vapor respectively. These liquid and vapor temperatures confirm the system being maintained at the saturation state during the experiments. Two thermocouples are embedded along the circumference of the heater close to the heating surface. The surface temperature is calculated by correcting the minor temperature drop due to the small distance between the heating surface and the thermocouple location using Fourier heat conduction equation. The internal pressure of boiling vessel is measured by a pressure transducer. The power input to the test heater is measured using a wattmeter. The boiling vessel is well insulated. Electrical signals from the thermocouples, pressure transducer and wattmeter are processed by a data acquisition system.

Fig. 3 shows schematic of the visualization of the boiling process. A high speed camera (Nikon D3) was used to take the photographs of the pool boiling on the outer surface of vertical heater inside the boiling vessel. The camera was positioned infront of the sight glass. A concentrated light source was placed infront of another sight glass opposite to the camera to give uniform illumination of the test heater.

## 3. Experimental procedure

### 3.1. Boiling

In order to start the boiling tests, the boiling vessel should be filled with the ammonia–water mixture. Before filling the chamber with the mixture, it was evacuated using a vacuum pump. The pressure of the boiling vessel was read on the logger display. Once the evacuation process was completed, the boiling vessel was filled with ammonia–water mixture. The amount of mixture was chosen so as to maintain a fixed level in all experiments. The test pressure was set in the logger. When the system was ready, the tests were started by giving a heat input to the test heater. The magnitude of the heat input was known from the wattmeter. All experimental runs were carried out with decreasing heat flux to avoid the hysteresis effect. Some runs were repeated twice and even thrice to ensure the reproducibility of the experiments.

Commercially available $NH_3$–$H_2O$ mixture with the mass concentration of 30% was used. The 30% mixture was diluted to 15% mass concentration of ammonia by adding measured quantity of distilled water. Subsequently, a measured quantity of $LiBr$–$H_2O$ solution of known concentration was added and the ternary mixture was heated to saturation temperature by giving heat input the rod heater. After equilibrium was reached, the saturation temperature, heater surface temperature was noted down for different heat flux and the set pressure was changed. The measurements
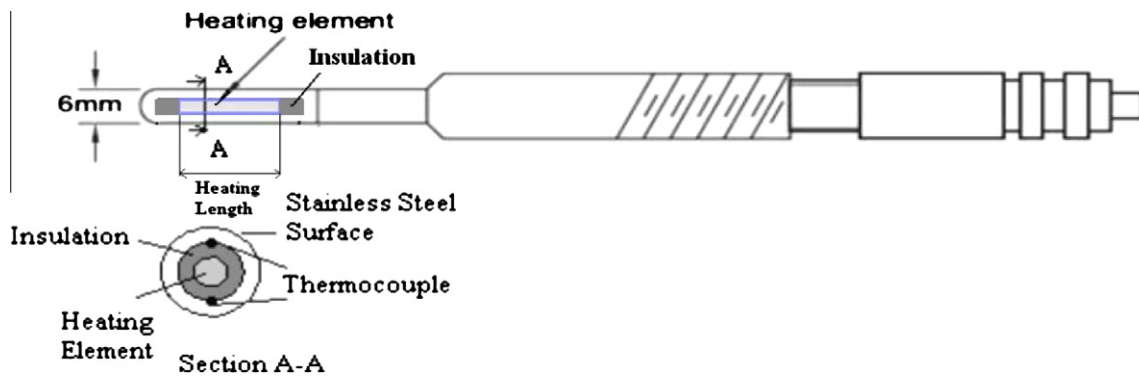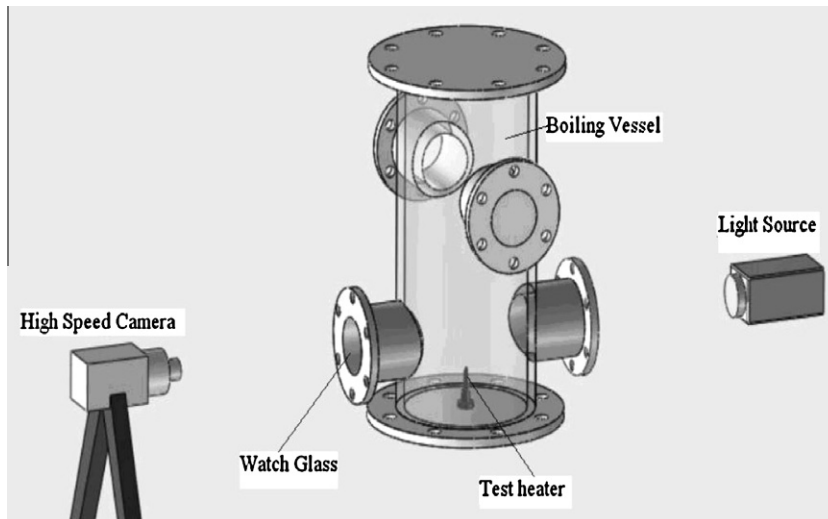


**Fig. 2.** Details of test heater.



**Fig. 3.** Visualization of boiling process.

were performed in the pressure range $p$ = 4–8 bar. The LiBr concentration of the solution was chosen in the range of 10–50% of mass ratio of LiBr in pure water. Lithium bromide salt is measured using a balance with a precision of ±0.01gm. Initial mass fractions are used in this paper to represent the concentration of the mixture.

### 3.2. Regulation and data collection

The set pressure is maintained constant throughout an experiment by the combination of the cooling water pump, pressure transducer and a proportional integral derivative (PID) pressure controller. The PID senses the pressure level in the boiling chamber through pressure transducer and compares it with the set value fed to it by the researcher. To go from a higher pressure level to a lower pressure level, the PID sends a signal to cooling water pump to open the suction line and pump water through the condenser coils. The digital temperature indicator reads the spontaneous temperatures. In total it reads three temperatures, of the one thermocouple in the test section, and of the one in the liquid and the one in the vapor. The digital wattmeter displays the power input to the heater. The Data Acquisition Unit logged data from all thermocouples as well as recorded the boiling vessel pressure, and heater supply power. Data was then transferred though the general programming interface bus data link to a computer. A custom MATLAB program was developed to save the results and chart the data as it was acquired.

## 4. Calculations

Heat input $Q$ is a known quantity as there can be no losses since the heater rod is completely immersed in the liquid. Then heat flux, $q = \frac{Q}{A}$, where $A$ is the area of the cylindrical test surface. $A = \pi d L$ where $d$ is the diameter of the heater rod and $L$ is the heating length of the heater rod. Heat transfer coefficient between the surface and the liquid is calculated by applying Newton's law of cooling

$$h = \frac{q}{T_w - T_s} \tag{1}$$

where $T_s$ is the saturation temperature of the liquid at the corresponding pressure, and $T_w$ is the surface temperature of the test surface.

## 5. Experimental uncertainty

All chrome alumel K type thermocouples used in this study have an accuracy of ±0.5% full scale. The pressure transducer has an accuracy of ±0.5 full scale. The power input to the heater is measured by an accurate digital power meter of accuracy ±1 W. The uncertainty in temperature measurement is ±1.25 °C. Uncertainty in length and diameter measurement is ±0.1 mm. The resulting uncertainty in the area of the heated surface is 1.74%. The Kline and McClintock [11] technique was used to estimate the uncertainty for the derived quantities.

Uncertainty in Percentage,

$$\omega_h = \left[ \left( \frac{\omega_Q}{Q} \right)^2 + \left( \frac{\omega_d}{d} \right)^2 + \left( \frac{\omega_L}{L} \right)^2 + \left( \frac{\omega_{T_w}}{T_w - T_s} \right)^2 + \left( \frac{\omega_{T_s}}{T_w - T_s} \right)^2 \right]^{1/2} \tag{2}$$

The resulting maximum uncertainty in the heat flux was 1.94%. The maximum uncertainty in the wall superheat values was 10.71%. The maximum uncertainty in the heat transfer coefficient was 10.86%.

## 6. Experimental results

To corroborate the validity of the achieved experimental data in the present experiments, measured boiling heat transfer for pure water are compared with nine well known correlations including Gorenflo [12], Stephan and Abdelsalam [13], Labantsov [14], Nishikawa et al., [15], Kutateladze [16], Kruzhilin [17], Mostinski [18], Rohsenow [19] and Cooper [20]. Fig. 4 presents the results for water at 4 bar pressure. For water all the correlations gave similar results. Stephan–Abdelsalam and Kutateladze correlations predict the present experimental data with good accuracy in the investigated range of high heat flux. Thus the experimental apparatus and method was found appropriate in performing the present mixture experiment. Thus the experimental apparatus and method was found appropriate in performing the present mixture experiment.

The mass fraction of ammonia and lithium bromide is defined as follows:

$$x_{NH_3} = \frac{m_{NH_3}}{m_{NH_3} + m_{H_2O}} \tag{3}$$

$$x_{LiBr} = \frac{m_{LiBr}}{m_{LiBr} + m_{H_2O}} \tag{4}$$

Heat transfer coefficient of three-component mixture varies as a function of the mixture composition and heat flux. So the heat transfer coefficient of ternary mixture needs three dimensional representation. Here two dimensional representation is used with concentration of ammonia kept constant. Figs. 5 and 6 represent the boiling curve and variation of heat transfer coefficient with heat flux for ammonia mass fraction of 0.30, and 0.15 respectively and at pressures 4–8 bar respectively. Note in the figures and table that the suffix '1' and '2', refer to the more- and moderate-volatile components, in the present ternary mixture, respectively. Thus, '1' refers to ammonia, '2' refers to water. 'LiBr' refers to non-volatile salt lithium bromide. Mixture composition is expressed in terms of mass fraction, such as $x_1$, $x_2$, and $x_{LiBr}$ in liquid phase.

Each line in Fig. 5 represents the boiling curve/heat transfer coefficient for one set of lithium bromide concentration for the solution with ammonia mass concentration of 30%. At 4 bar pressure, heat transfer coefficient increases with addition of LiBr, as the concentration of lithium bromide increases, heat transfer coefficient increases remarkably for the solution of constant ammonia
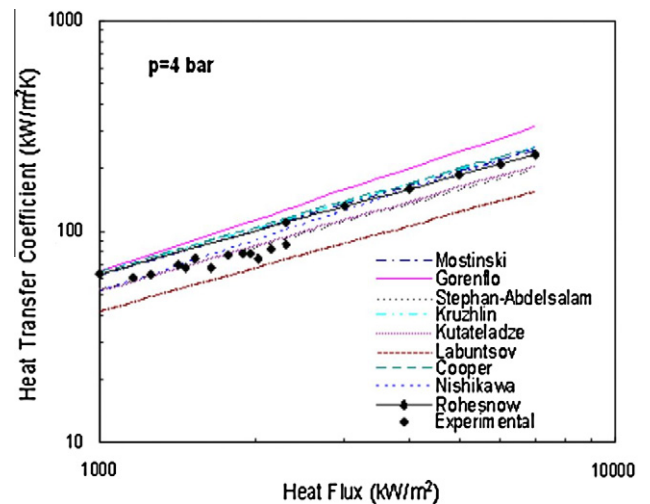


**Fig. 4.** Comparison between measured and predicted heat transfer coefficient for water at 4 bar pressure.
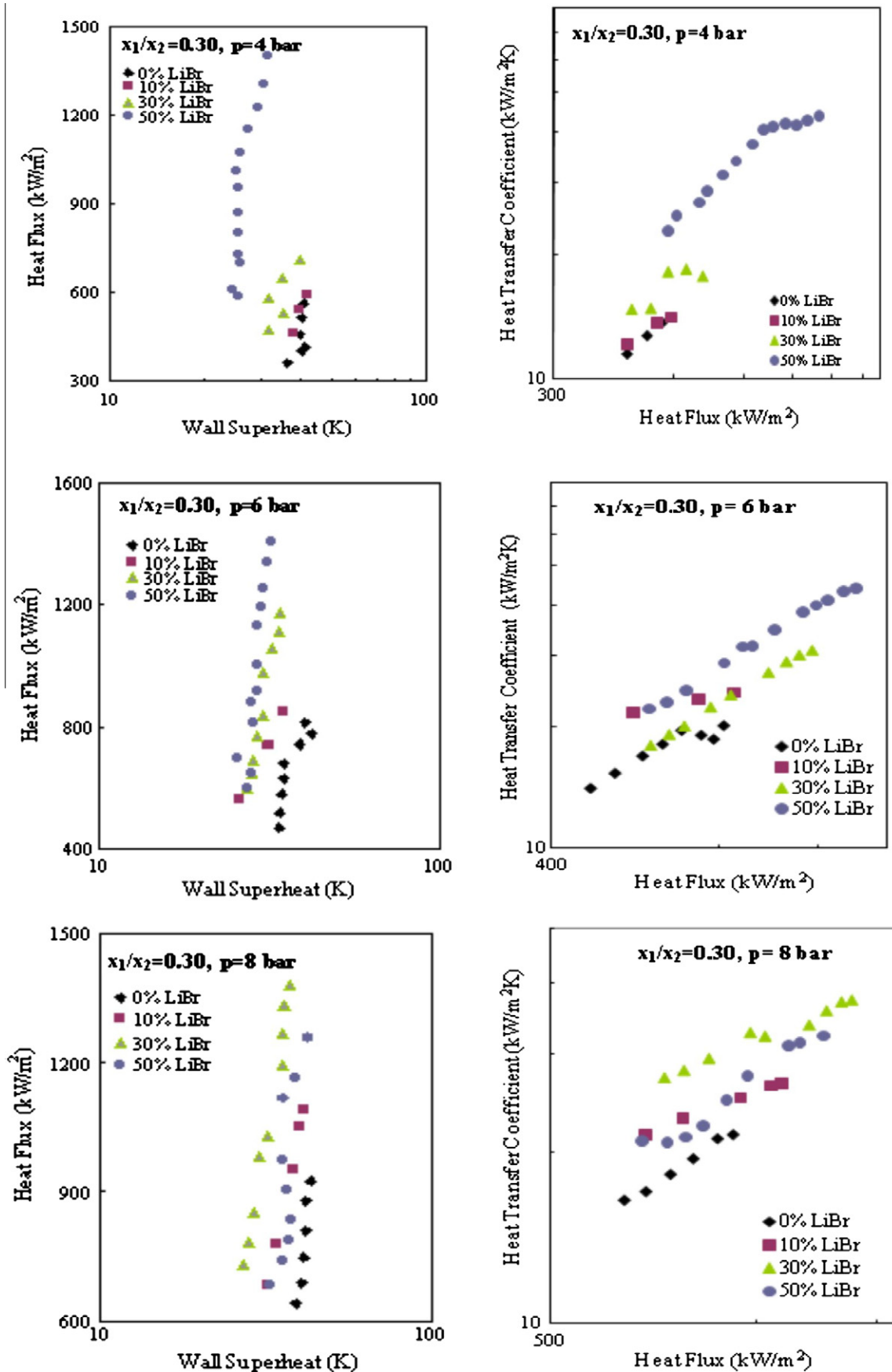
Fig. 5. Boiling curve and variation of heat transfer coefficient with heat flux for 30% $NH_3$ at different pressures with varying concentration of LiBr.

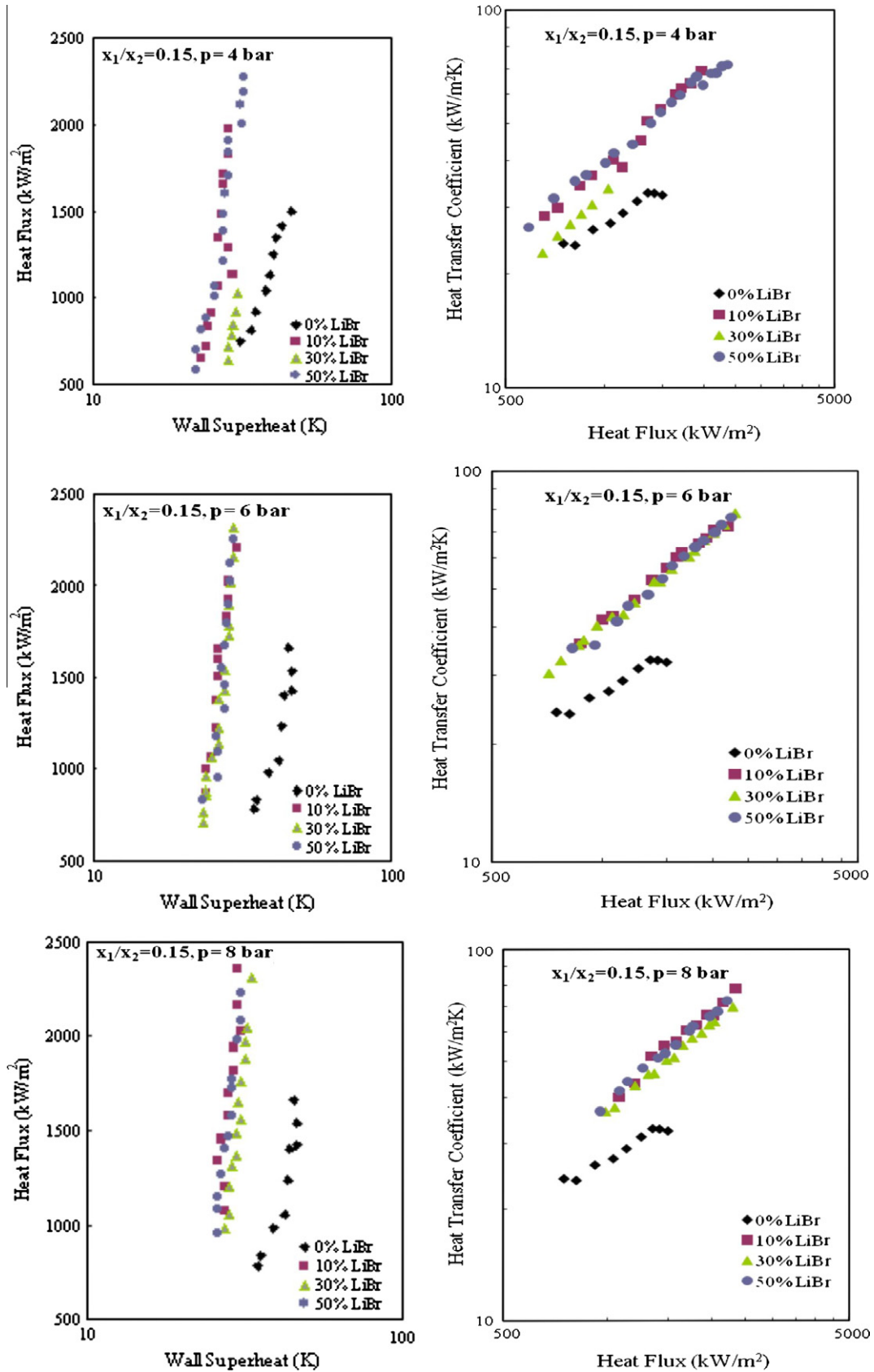**Fig. 6.** Boiling curve and variation of heat transfer coefficient with heat flux for 15% NH$_3$ at different pressures with varying concentration of LiBr.

concentration. This could be due to the easy departure of the bubble, smaller bubble size, shorter departure period by the dense

salt molecules near the heated surface. The effect of increase in salt concentration becomes weak at high pressures. At high pressure

bubbles are emitted vigorously all over the heated surface. Salt molecules cannot reach the heated surface due to the bubble agitation and vigorous bubble departure near the heated surface. Although the addition of lithium bromide increases the boiling heat transfer coefficient in the aqua ammonia solution with initial ammonia concentration of 15%, the increase in concentration of lithium bromide does not seem to be effective as seen in Fig. 6. This is attributed to increase in viscosity of the solution with increase in lithium bromide salt concentration at low ammonia mass concnetration.

The present results are somewhat contrary to expectations. The addition of salts increases the viscosity of the $NH_3$–$H_2O$ mixture resulting in decrease in film heat and mass transfer coefficients. Reiner and Zaltash [21] reported that the dynamic viscosity of $NH_3$–$H_2O$–$LiBr$ ternary solution was seven times larger than the $NH_3$–$H_2O$ binary solution. As convection plays a major role in heat



(a) Without Salt, q = 563 kW/m$^2$

(b) $x_{LiBr}$ =0.10, q = 555 kW/m$^2$

(c) $x_{LiBr}$ =0.30, q = 555 kW/m$^2$

(d) $x_{LiBr}$ =0.50, q = 624 kW/m$^2$

(e) Without Salt, q = 724 kW/m$^2$

(f) $x_{LiBr}$ =0.10, q = 772 kW/m$^2$

(g) $x_{LiBr}$ =0.30, q = 719 kW/m$^2$

(h) $x_{LiBr}$ =0.50, q = 691 kW/m$^2$

p = 4 bar

(i) Without Salt, q=577 kW/m$^2$

(j) $x_{LiBr}$ =0.10, q = 772 kW/m$^2$

(k) $x_{LiBr}$ =0.30, q = 583 kW/m$^2$

(l) $x_{LiBr}$ =0.50, q = 564 kW/m$^2$

(m) Without Salt, q=788 kW/m$^2$

(n) $x_{LiBr}$ =0.10, q = 761 kW/m$^2$

(o) $x_{LiBr}$ =0.30, q = 747 kW/m$^2$
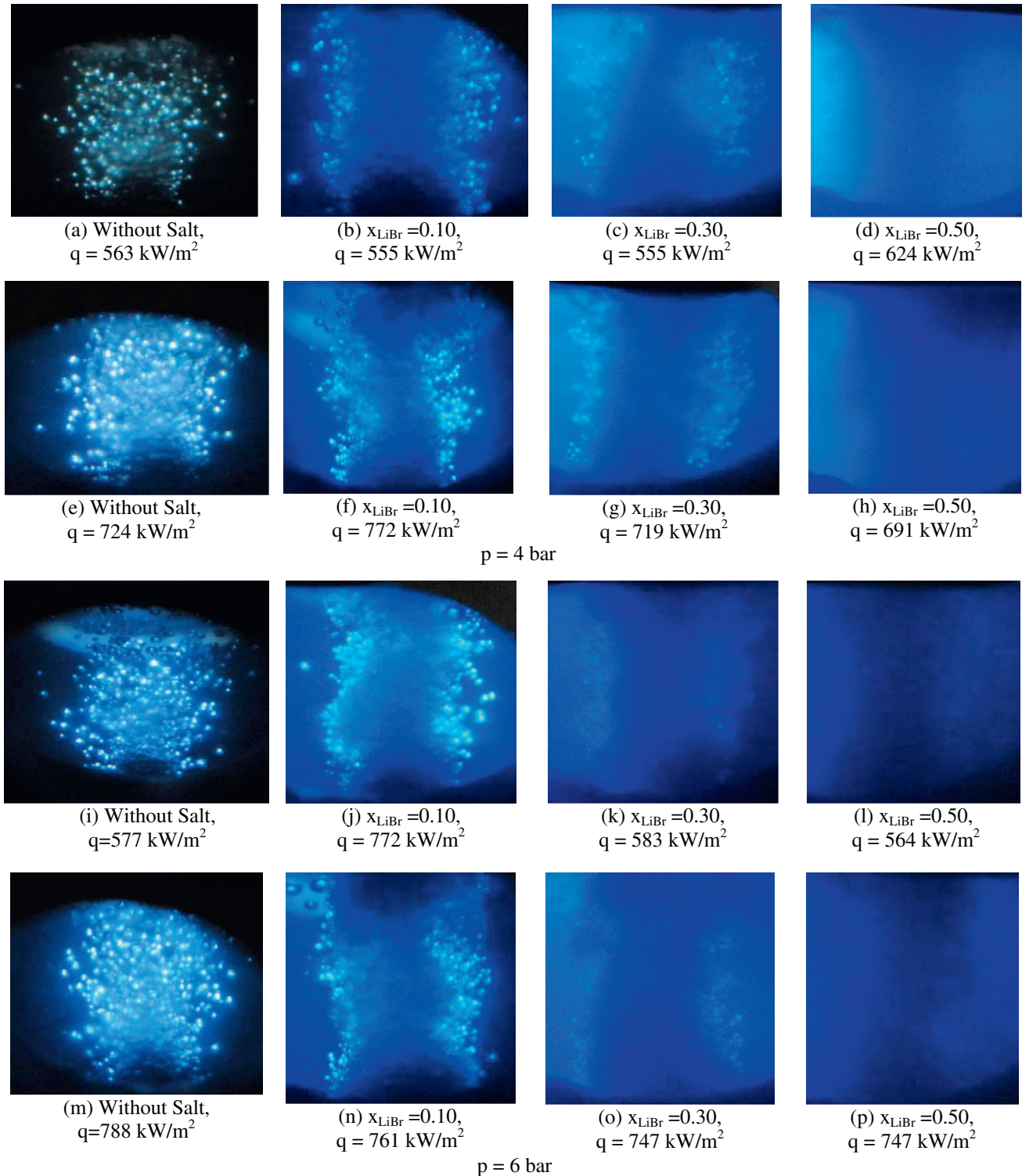
(p) $x_{LiBr}$ =0.50, q = 747 kW/m$^2$

p = 6 bar

**Fig. 7.** Visual record of boiling phenomena in ammonia–water–lithium bromide mixture for $x_{NH_3}$ = 0.30 at different pressure and concentration of lithium bromide.

(q) Without Salt,
q=585 kW/m$^2$

(r) $x_{LiBr}$ =0.10,
q = 585 kW/m$^2$

(s) $x_{LiBr}$ =0.30,
q = 532 kW/m$^2$

(t) $x_{LiBr}$ =0.50,
q = 574 kW/m$^2$

(u) Without Salt,
q=760 kW/m$^2$

(v) $x_{LiBr}$ =0.10,
q = 741 kW/m$^2$

(w) $x_{LiBr}$ =0.30,
q = 719 kW/m$^2$

(x) $x_{LiBr}$ =0.50,
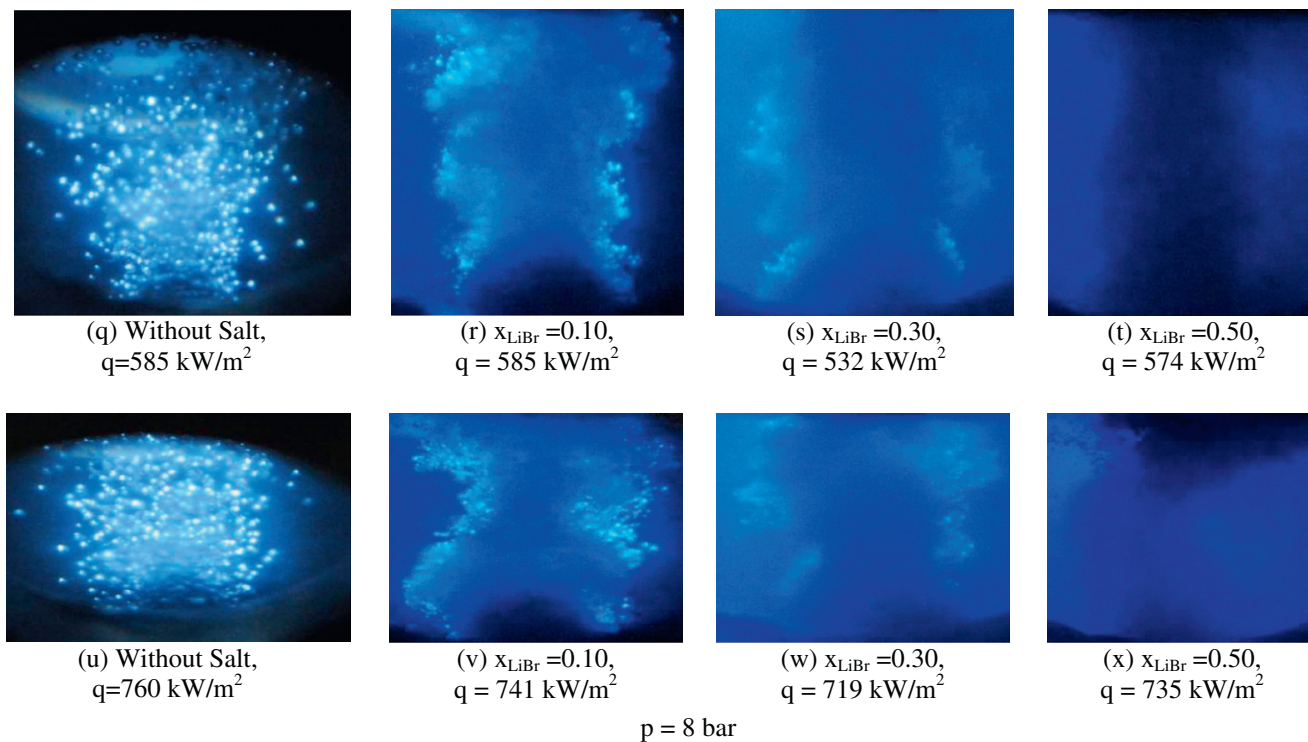q = 735 kW/m$^2$

p = 8 bar

**Fig. 7** (*continued*)

transfer during pool boiling, with such a substantial increase in viscosity, salts are expected to degrade heat transfer characteristic during pool boiling. Then increase in boiling heat transfer may be due to changes in the other thermophysical properties of the ternary salt solution.

Upon adding salt to the $NH_3$–$H_2O$ mixture, the surface tension is expected to reduce. The surface tension depression will enhance the boiling heat transfer remarkably. Inoue et al. [9] observed a significant decrease in surface tension and significant increase in boiling heat transfer in ethanol/water mixture by the addition of surfactant up to a surfactant concentration of 1000 PPM. Systematic experimental measurements of dynamic surface tension and contact angle are required to explain the complex dependence of concentration of LiBr salt additive on boiling heat transfer observed in this work.

Thermal conductivity of the salt solution is expected to be high. Since fluid conduction in microlayer evaporation under the bubble as well as in reformation of thermal boundary layer at the nucleation site plays a major role in heat transfer during pool boiling, with increase in thermal conductivity, ternary solutions are expected to enhance heat transfer characteristic during pool boiling. Sliding of bubbles is also important in pool boiling, especially in the present work in which a vertical heater is used, where again conduction mechanism, the increase in thermal conductivity is expected to enhance heat transfer during boiling.

Another possible explanation for the behavior observed could be provided by nucleation theory as speculated by Lowery and Westwater [22]. With the addition of small particles or large molecules, additional interfacial tensions becomes important, namely the particle-liquid–vapor system. This could create a synthetic nucleus promoting vapor generation on the hot solid and/or in surrounding superheated liquid. Higher concentrations resulted in the deposition of a thin film on the heater surface and a decrease in nucleate boiling heat transfer was observed. At what point the degradation mechanisms outweigh any enhancement remains

unclear. This may explain the importance of LiBr concentration observed in this study.

## 7. Bubble dynamics

It is known that nucleate boiling is characterized by the formation of vapor bubbles from fixed sites randomly distributed on a heating surface. Aspects of the boiling heat transfer mechanisms on heated surfaces remain unclear due to the highly complex nature of boiling and difficulty in measurements such as the determination of key boiling parameters such as bubble departure diameter, velocity, frequency, and active nucleation site density study. Previous studies have employed several photographic techniques to determine the above-stated bubble dynamic data. Few of them have applied the data to predict each component of the total heat flux (latent heat, natural convection, and microconvection) as well as to validate their boiling models. In spite of the vast amount of effort devoted to boiling studies, there is still no definitive, comprehensive explanation for the actual mechanism of bubble nucleation, growth, and departure that controls the heat transfer field in the vicinity of the nucleation site. Experimental data concerning the details of these processes are lacking. The rate of bubble growth and subsequent bubble motion has tremendous influence on heat transfer and the precipitation of non-volatile species. In the present investigation, bubble dynamics in $NH_3$–$H_2O$ and $NH_3$–$H_2O$–LiBr are compared. A high speed, digital camera is used for capturing visual observations of bubbles. High intensity light is used to illuminate the nucleating cavities and suitable zoom lenses are used to focus on them.

Bubble nucleation parameters were not clearly measurable, due to the much greater density of nucleation sites on the heater surface considered in this work. The exact timing of bubble departure could not be noted, as the growing bubbles always moved from their nucleation sites while still being attached to the surface,

either by merger with a larger neighboring bubble or by sliding due to a buoyancy-driven bulk flow. The contact angle, the site density and the bubble frequency could not be measured due to the above said reason. Isolation of single bubble on the surface could not be done for study.

Fig. 7a–x shows the flow situation on the heated surface at different pressures, change of flow aspect with heat flux and change with the mass fraction of lithium bromide for constant ammonia concentration of 0.30. Fig. 7a–d shows the bubble dynamics at 4 bar pressure and at low heat flux. Bubble diameter decreases with the addition of LiBr and this decrement increases with increase in LiBr concentration. At high concentration of LiBr boiling becomes violent, frequency of bubble formation increases, the bubbles merge to form a continuous vapor plume. At higher pressures bubble coalesce with difficulty. Similar observations are made at higher heat flux.

## 8. Conclusion

Bubble dynamics and pool boiling heat transfer to $NH_3$–$H_2O$ and $NH_3$–$H_2O$–LiBr solutions at different pressure, heat flux and concentrations were studied. Nucleate boiling in multicomponent mixtures is a complex conjugate process, and it depends on a variety of factors. However, the primary heat transfer is by evaporation and its efficiency is directly related to nucleation site density and bubble dynamics. Phenomenological insights can be obtained from a visual observation of $NH_3$–$H_2O$ and $NH_3$–$H_2O$–LiBr boiling at high heat flux. In comparison to that in $NH_3$–$H_2O$, boiling in $NH_3$–$H_2O$–LiBr solution was more vigorous and characterized by clusters of small-sized, more regularly shaped bubbles that had higher departure frequency. One may conclude that LiBr promoted activation of nucleation sites. Besides the effects discussed above the bulk concentration of LiBr and its chemistry (ionic nature and molecular weight), dynamic surface tension, surface wetting or contact angle, surface adsorption and desorption, and foaming should be considered to have a significant influence. A direct correlation of the heat transfer with suitable descriptive parameters for these effects is difficult due to the complex nature of the problem.

## References

[1] R. Radermacher, Ph.D. thesis, Technical University of Munich, Germany, 1981.
[2] M. McLinden, R. Radermacher, An experimental comparison of ammonia–water and ammonia–water–lithium bromide mixtures in an absorption heat pump, ASHRAE Trans. 91 (2B-2) (1985) 1837–1846.
[3] M. Peters, R. Greb, O. Korinth, C.A. Zimmermann, Vapor–liquid-equilibria in the system $NH_3$–$H_2O$–LiBr, part I: measurements in the range $T$ = 303–423 K and $p$ = 0.1–1.5 MPa, J. Chem. Eng. Data 40 (4) (1995) 769–774.
[4] R. Peters, C. Korinth, J.U. Keller, Vapor–liquid equilibria in the system $NH_3$ +$H_2O$+LiBr. 2. Data correlation., J. Chem. Eng. Data 40 (4) (1995) 775.
[5] Yuyuan Wu, Yan Chen, Tiehui Wu, Experimental researches on characteristics of vapor–liquid equilibrium of $NH_3$–$H_2O$–LiBr system, Int. J. Refrig. 29 (2006) 328–335.
[6] T. Inoue, M. Monde, Y. Teruya, Pool boiling heat transfer in binary mixtures of ammonia and water, Int. J. Heat Mass Transfer 45 (2002) 4409–4415.
[7] H. Arima, M. Monde, Y. Mitsutake, Heat transfer in pool boiling of ammonia water mixture, Heat Mass Transfer 39 (2003) 535–543.
[8] Y. Fujita, M. Tsutsui, Heat transfer in pool boiling of binary mixtures, Int. J. Heat Mass Transfer 37 (1994) 291–302.
[9] T. Inoue, Y. Teruya, M. Monde, Enhancement of pool boiling heat transfer in water and ethanol/water mixtures with surface–active agent, Int. J. Heat Mass Transfer 47 (2004) 5555–5563.
[10] M. Jamialahmadi, A. Helalizadeh, H. Müller-Steinhagen, Pool boiling heat transfer to electrolyte solutions, Int. J. Heat Mass Transfer 47 (4) (2004) 729–742.
[11] S.J. Kline, F.A. McClintock, Describing uncertainties in single-sample experiments, Mech. Eng. (1953) 3.
[12] D. Gorenflo, VDI-Heat Atlas, 1997.
[13] K. Stephan, M. Abdelsalam, Heat transfer correlations for natural convection boiling, Int. J. Heat Mass Transfer 23 (1980) 73–87.
[14] D.A. Labuntsov, Heat transfer problems with nucleate boiling of liquids, Thermal Eng. 19 (9) (1972) 21–28.
[15] K. Nishikawa, Y. Fujita, H. Ohta, S. Hidaka, Effect of the surface roughness on the nucleate boiling heat transfer over the wide range of pressure, in: Proc. 7th Int. Heat Transfer Conf. vol. 4, 1982, pp. 61–66.
[16] Kutateladze, Heat Transfer and Hydrodynamic Resistance: Handbook, 1990.
[17] G.N. Kruzhlin, Free convection transfer of heat from a horizontal plate and boiling liquid, Dokl. AN SSSR (Rep. USSR Acad. Sci.) 58 (8) (1947) 1657–1660.
[18] I.L. Mostinski, Application of the rule of corresponding states for calculation of heat transfer and critical heat flux, Teploenergetika 4 (1963) 66.
[19] W.M. Rohsenow, A method of correlating heat transfer data for surface boiling of liquids, Trans. ASME 74 (1952) 969–976.
[20] M.G. Cooper, Saturation nucleate pool boiling e a simple correlation, in: IChemE Symposium Series, vol. 86, 1984, pp. 786–793.
[21] R.H. Reiner, A. Zaltash, Densities and viscosities of ternary ammonia/water fluids, in: ASME Winter Annual Meeting, New Orleans, November 28–December 3, 1993.
[22] A.J. Lowery Jr., J.W. Westwater, Heat transfer to boiling methanol–effect of added agents, Ind. Eng. Chem. 49 (9) (1957) 1445–1448.